의공학회지 : 제17권, 제2호, 1996
J. of KOSOMBE : Vol. 17, No. 2

연 구 논 문
96 - 17 - 2 - 02

Imaging Characteristics of Plastic Scintillating Fiber Screens for Digital Mammography

Won-Young Choi*, James K. Walker*, Zhenxue Jing**

=Abstract=

A scanning slot digital mammography system using a plastic scintillating fiber screen (SFS) is currently being developed. To improve the x-ray interaction efficiency and absorption efficiency of an SFS, high Z elements can be added into the scintillating fiber core. In this paper, we investigated theoretically the zero spatial frequency detective quantum efficiency, DQE(0), and modulation transfer function, MTF(f), of three 2 cm thick SFSs made of polystyrene, polystyrene loaded with 5% by weight of lead, and polystyrene loaded with 10% by weight of tin scintillating fibers. X-ray interaction efficiency, scintillating light intensity distributions and line spread functions were generated using Monte Carlo simulation. DQE(0) and MTF(f) were computed for x-ray energies ranging from 15 to 50 keV. Loading high Z elements into the SFS markedly increased the DQE(0). For x-ray energies used for mammography, DQE(0) values of both high Z element loaded SFSs are about a factor of three higher than the DQE(0) of an Min-R screen. At mammographic x-ray energies, MTF(f) values of all three SFSs are greater than 50% at 25 lp/mm spatial frequency, and were found to be dominated by the 20 μm individual scintillating fiber diameter used. The results show that both high DQE(0) and spatial resolution can be achieved with the high Z element loaded SFSs, which make these SFSs attractive for use in a scanning slot detector for digital mammography.

Key words : Digital mammography, Plastic scintillating fiber, Swank factor, Detective quantum efficiency, Modulation transfer function.

INTRODUCTION

Current designs of scanning slot detectors for digital mammography use Gd_2O_2S : Tb rare earth phosphor screen optically coupled to charge-coupled devices (CCD)[1), 2)]. The two main limitations of these detectors stem from the use of this phosphor screen. First, using a phosphor screen coupled to CCDs will inevitably reduce the spatial resolution compared to the modern mammography screen-film combination, for which a single emulsion film is used in combination with a single back-intensifying screen. Second, the afterglow (slow scintillation decaying component) nature of the Gd_2O_2S : Tb phosphor reduces these scanning slot detectors' modulation transfer function, MTF(f), where f is the spatial frequency.

A possible approach is to use a plastic scintillating fiber screen (SFS) as the x-ray-to-light converter in a scanning slot detector for mammography. An SFS is composed of individual plastic scintillating fibers fused together with their axes aligned to the direction of the incident x-ray beam. Because the scintillation light dispersion is limited to the individual fiber diameter, a relatively thick SFS can be used to increase its x-ray interaction efficiency without degrading spatial resolution. The scintillation decay time of a plastic scintillator is only a few nanoseconds which guarantees no loss of MTF(f) when an SFS is used in a scanning detector. In this paper, we investigated the effect of loading high Z elements including tin and

*Nanoptics, Inc., Gainesville, FL 32609, U.S.A.
**Department of Rediology, University of Florida, U.S.A.
통신저자 : 최원영 Tel. (1-352-337-1271)

lead on the zero spatial frequency detective quantum efficiency, DQE(0), and MTF(f) of the plastic SFSs.

THEORY

1. Zero spatial frequency detective quantum efficiency

Noise due to the x-ray conversion processes within an x-ray detector based on the phosphor screens has been characterized by the Swank factor, A_S[3]. Calculation of A_S can be performed from the phosphor screen scintillation light output intensity distribution when x-rays of monoenergetic energy incident on the phosphor screen[4),5)]. In an SFS, emitted scintillation light is collected and transmitted to the SFS output due to the total reflection principle. The number of light photons exiting the SFS is proportional to the total number, N, of light photons emitted per absorbed x-ray, and is independent on the depth of x-ray interaction within the SFS. In this study, the emitted light intensity distribution, P(N), was therefore used to obtain the Swank factor as given by[4)].

$$A_S = \frac{m_1^2}{m_0 m_2} \tag{1}$$

where the ith moment of P(N) is defined as

$$m_i = \sum_{0}^{N_{max}} P(N) N^i \tag{2}$$

For monoenergetic incident x-ray energy, it has been shown that the zero spatial frequency detective quantum efficiency, DQE(0), of a phosphor screen is given by[4),6)].

$$DQE(0) = \eta \cdot A_S \tag{3}$$

where η is the x-ray interaction efficiency, which is the fraction of incident x-rays which interact within the phosphor screen.

2. Modulation transfer function

Two stages in the image formation using an SFS determine the screen spatial resolution. First, x-ray interactions with the SFS include Compton scattering, coherent scattering, and photoelectric effect. An incident x-ray undergoes single or multiple interactions before being totally absorbed or scattered out of the SFS. This leads to the spread of incident x-ray energy deposition from the primary interaction site. Second, the emitted light is collected by the scintillating fibers and transmitted to the SFS output side. The MTF(f) of an SFS, $MTF_S(f)$, is therefore given by

$$MTF_S(f) = MTF_E(f) \cdot MTF_0(f) \tag{4}$$

where, $MTF_E(f)$ is the spatial resolution of the incident x-ray energy spread, and $MTF_0(f)$, optical MTF, is the spatial resolution of the scintillation light spread. For an SFS made of uniformly packed scintillating fibers of same diameter, d, $MTF_0(f)$ is given by

$$MTF_0(f) = \frac{\sin(\pi \cdot f \cdot d)}{\pi \cdot f \cdot d} \tag{5}$$

METHODS

1. Plastic scintillating fiber screens

A schematic of a slot shaped plastic scintillating fiber screen (SFS) designed for mammography is shown in Figure 1. Plastic scintillators have much lower x-ray interaction cross sections than phosphor screens used for mammography. In order to produce a high x-ray interaction efficiency, the thickness of a plastic SFS should be maximized. To take account of the parallax effect as a result of this relatively larger thickness, the fiber axes are arranged to be parallel to the direction of the incident x-rays, as shown in Figure 1.

At mammographic x-ray energy range, adding a small amount of high Z element into the plastic scintillating fiber core material not only improves the SFS x-ray interaction efficiency, but also increases the SFS photoelectric effect cross section. However, addition of the high Z elements in the plastic scintillator also leads to a decreased scintillation light output (or quenching). In this study, the imaging properties of two high Z element loaded SFSs were compared to that of a pure polystyrene (PS) based plastic SFS, SFS:PS. One SFSs contains 10% by weight of tin element in its scintillating fiber core material, SFS:Sn. The other is loaded with 5% by weight of lead, SFS:

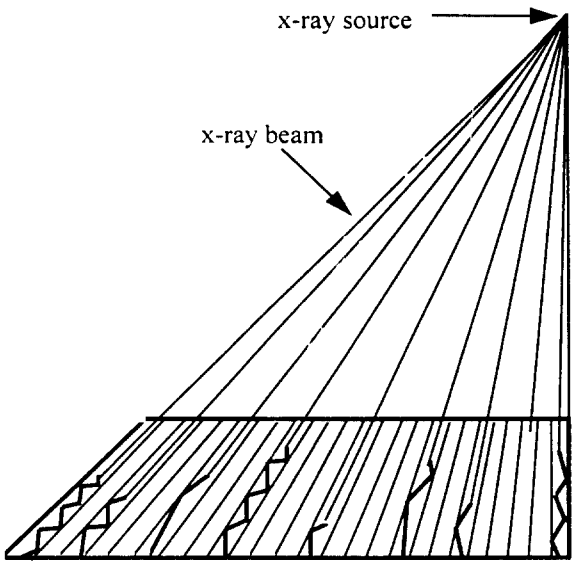

Fig. 1. A parallax corrected, slot shaped plastic scintillating fiber screen (SFS)

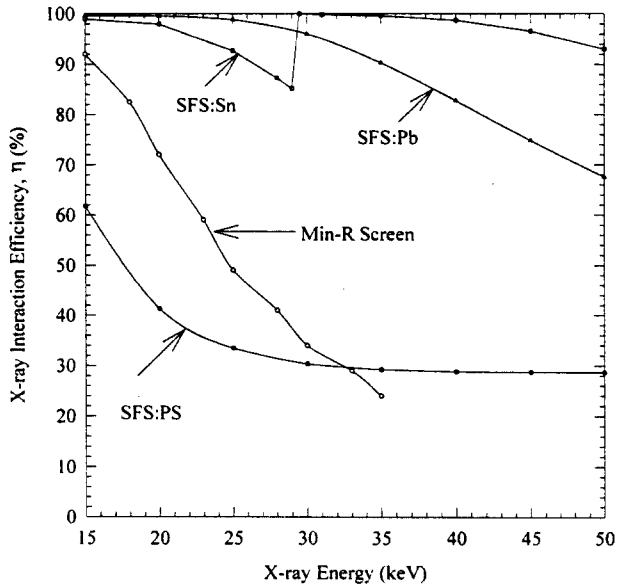

Fig. 2. X-ray interaction efficiency for three SFSs and for a Kodak Min-R screen

Pb. The energy conversion efficiency, ε, of all three SFSs is 4.5%. There is an 15% light loss (L) due to the reabsorption of the scintillating dye in each SFS. The fraction, q, of the scintillation light lost due to quenching is 20% for both high Z element loaded SFSs[7,8]. All three slot shaped SFSs investigated were 2cm in thickness, 0.8cm wide and 20cm long. The diameter, d, of the scintillating fibers used was 20μm.

2. Monte Carlo simulations

In all simulations, monoenergetic x-rays from a point source were normally incident on the SFS. Three x-ray interaction processes with the SFSs were included : Compton scattering, coherent scattering, and photoelectric effect. Scattered x-rays can either interact again in a remote location within the SFS, or escape without being absorbed. For tin and lead loaded SFSs, characteristic x-rays could be emitted following photoelectric interactions. The Compton recoil electrons, photoelectrons and Auger electrons were assumed to deposit their energies in the x-ray interaction sites. X-ray interaction efficiency, η, was computed as the ratio of the number of incident x-rays interacted within the SFS to the total number of incident x-rays (history) used for each simulation.

In the Swank factor analysis, total x-ray energy deposited, Ed, from each interacted incident x-ray was generated. Ed varies due to the variation in the x-ray absorption processes. For each Ed, the average number of light photons emitted, $\overline{N}$, is given by

$$\overline{N} = \varepsilon \cdot (1-L) \cdot (1-q) \cdot \frac{Ed}{2.34} \qquad (6)$$

We took the wavelength of all emitted light photons to be 530 nm (2.34 eV). The conversion from Ed to the number, N, of light photons emitted is also a random process which is described by a Poisson distribution with mean equals to $\overline{N}$. In the simulation, for each $\overline{N}$ computed using equation (6), N was generated using the rejection sampling method[9]. The resultant emitted light intensity distribution, P(N), was used to calculate the Swank factor using equations (1) and (2).

The point spread functions, PSF_E, of the spread of x-ray energy deposition were generated for monoenergetic x-ray energies from 15 to 50 keV. The SFS was divided into a two dimensional array composed of squares of 5μm^2 size. Total energy deposition, $E_{i,j}$, inside a square centered at (x_i, y_j) from the normally incident pencil beam of x-rays was calculated. By definition, we have $PSF_E = E_{i,j}$. The line spread function, LSF_E, of this deposited energy spread was calculated by integrating the point spread function in one

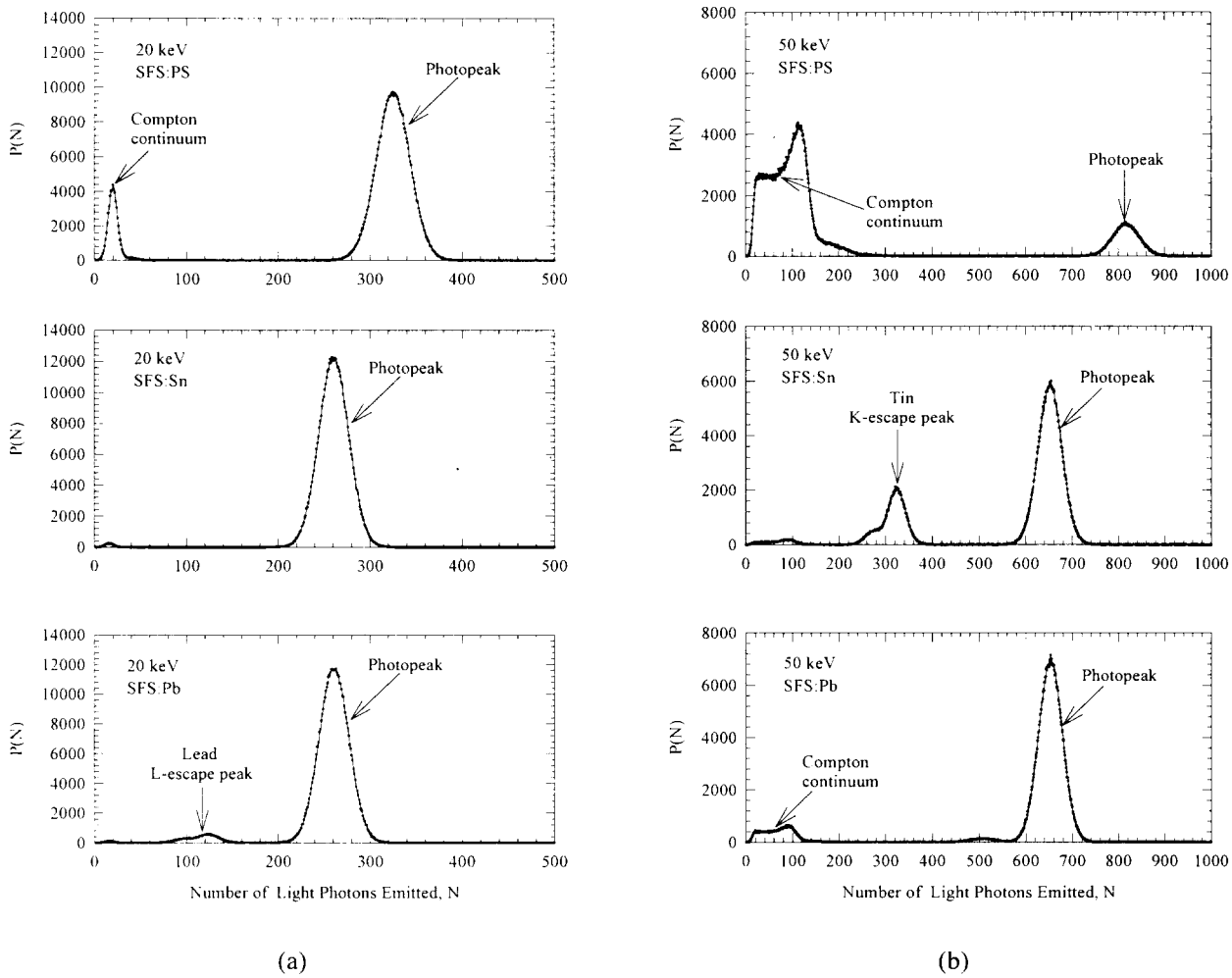

Fig. 3. Emitted light intensity distributions for three SFSs at (a) 20 and (b) 50 keV x-ray energies

dimension. LSF_E is therefore given by

$$LSF_E = \sum_{j=-\infty}^{\infty} E_{L,j} \qquad (7)$$

MTF_E was obtained from the modulus of the Fourier transform of the LSF_E.

RESULTS AND DISCUSSION

1. Zero spatial frequency DQE

1) X-ray interaction efficiency

The x-ray interaction efficiency is shown in Figure 2 as a function of incident x-ray energy for the three SFSs and a Kodak Min-R screen.[10] Loading high Z elements into a plastic SFS significantly improved its x-ray interaction efficiency. X-ray interaction efficiency of SFS : Sn or SFS : Pb was higher than the x-ray interaction efficiency of the Kodak Min-R screen.

2) Swank factor

Figures 3(a) and 3(b) show the emitted light intensity distributions, P(N), for the SFSs at 20 and 50 keV x-ray energies. P(N)s of the SFS : PS are always composed of a photopeak and a Compton continuum. P(N)'s of the high Z element loaded SFSs are dominated by the photopeak. The photopeaks of the high Z element loaded SFSs shift to a smaller N value than that of the SFS : PS photopeak. This is due to the quenching of scintillation light by the addition of high Z elements in the SFS.

Figure 4 shows the calculated A_S of the SFSs as a function of incident x-ray energy. The measured A_S

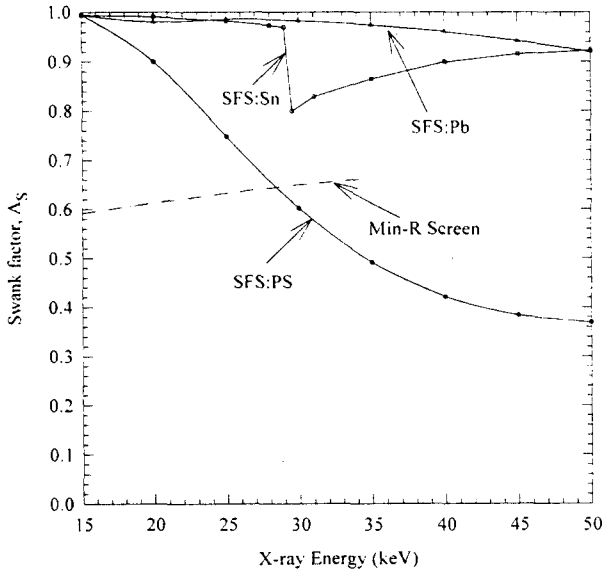

Fig. 4. Swank factor, A_S, as a function of incident x-ray energy for three SFSs and an Min-R screen

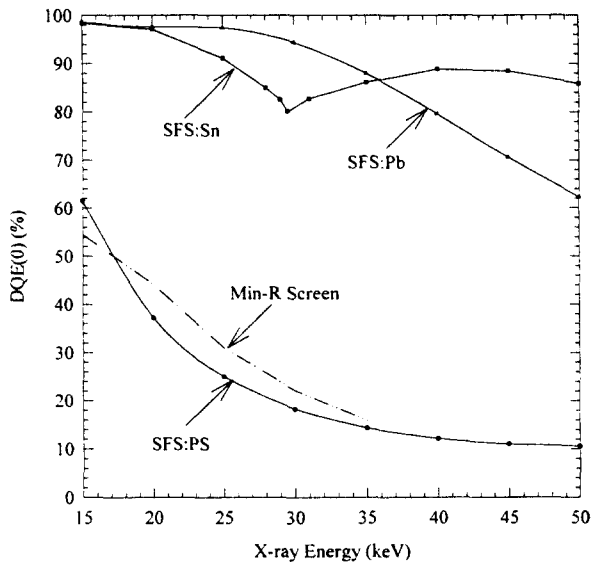

Fig. 5. DQE(0) plotted as a function of incident x-ray energy for three SFSs and an Min-R screen

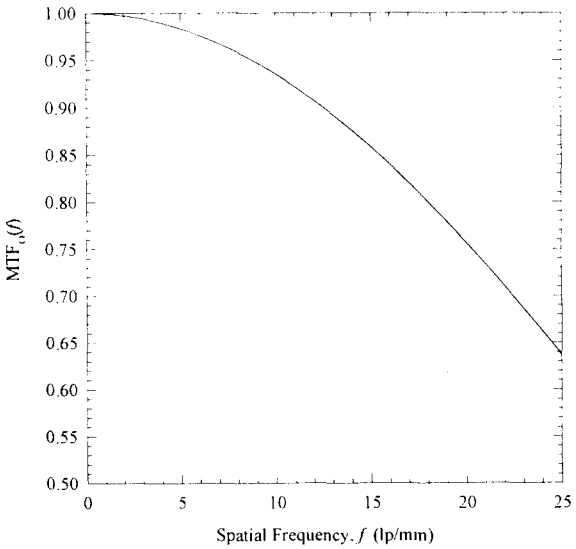

Fig. 6. $MTF_0(f)$ for an SFS with individual fiber diameter of 20μm

of an Min-R screen[11] is also shown in Figure 4. A_S of the SFS : PS decreases quickly as x-ray energy increases which is due to the reduced photoelectric interaction cross section with increasing incident x-ray energy. Because P(N)'s of SFS : Pb are dominated by the photopeak, A_S of the SFS : Pb is close to unity from 15 to 50 keV. At x-ray energies below the tin K-edge (29.2 keV), A_S of the SFS : Sn is also close to unity. Although it drops abruptly just above the tin K-edge, A_S of SFS : Sn increases as x-ray energy increases further. The results show that Swank factors of both the SFS : Pb and SFS : Sn are significantly higher than that of an Min-R screen.

3) Zero spatial frequency DQE

Figure 5 shows the DQE(0) as a function of incident x-ray energy for the three SFSs. The DQE(0) of an Min-R screen is also shown in Figure 5. Loading high Z elements significantly improves the DQE (0) of the plastic SFS. DQE(0) of the SFS : Pb ranges from about 99% to 62% from 15 to 50 keV, and is primarily determined by its x-ray interaction efficiency. DQE(0) of the SFS : Sn is greater than 80%. In the 20 to 30 keV x-ray energy range, DQE(0) of the high Z element loaded SFSs is a factor of three higher than the DQE(0) of the Min-R screen.

2. Modulation transfer functions

1) Optical MTF

Figure 6 shows the $MTF_0(f)$ for an SFS made of scintillating fibers of 20μm diameter. $MTF_0(f)$ values are 0.98, 0.93, 0.85 and 0.75 at 5, 10, 15 and 20 lp/mm, respectively.

2) Energy deposition line spread function

Figure 7 shows the calculated LSF_E curves at 20, 35, and 50 keV incident x-ray. The major difference

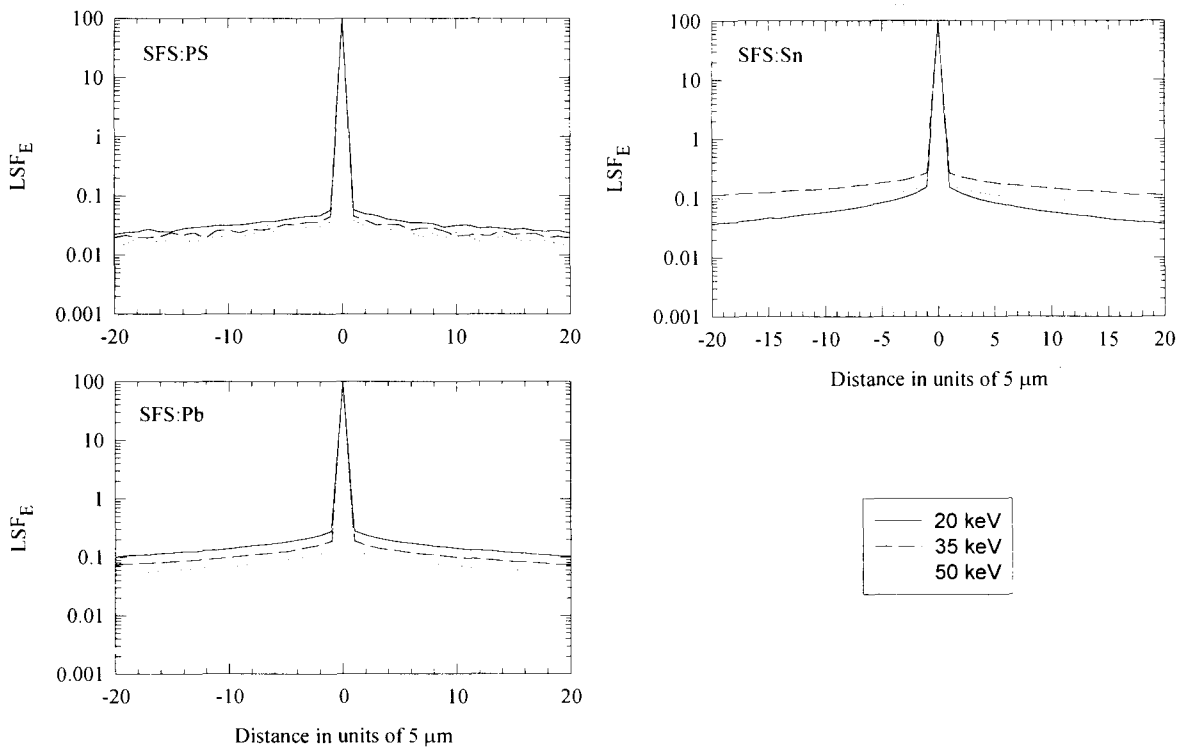

Fig. 7. LSF_E curves plotted for three SFSs at 20, 35 and 50 keV incident x-ray energies

in the LSF_E curves of the three SFSs is shown in the tails of these curves. LSF_E of the SFS : PS shows little dependence on the incident x-ray energy, and has the smallest spread among the three SFSs. The reason is that scattered x-rays carry most of the incident x-ray energy and has the highest probability to escape in the SFS : PS. For SFS : Pb, the tail in its LSF_E curve becomes smaller as the x-ray energy increases. This is mainly due to the increased energy transfer to the photoelectrons which deposit their energies at the primary interaction site. LSF_E of SFS : Sn at 20 keV is better than the LSF_E of SFS : Pb at all incident x-ray energies. However, the reabsorption of tin K x-rays causes large degradation in the resultant LSF_E at 35 keV x-ray energy. Similar to the SFS : Pb, the tail in the LSF_E of the SFS : Sn at 50 keV is smaller than at 35 keV.

It was noted that the assumption of electrons depositing their energies in the x-ray interaction sites is reasonable for Compton recoil electrons (less than 9 keV electron energy) and Auger electrons. However, the energy of the photoelectron increases with increasing x-ray energy at incident x-ray energies greater than the K- or L-edge of the high Z elements. A 15 keV photoelectron from a 20 keV x-ray interaction can travel a distance of about 5 μm before its energy being completely absorbed. Thus, for mammographic x-ray energies, the photoelectron range only has a small effect on the calculated LSF_E curves shown in Figure 7.

3) Scintillating fiber screen MTF

Figure 8 shows the $MTF_S(f)$ curves of the three SFSs at 20, 35 and 50 keV incident x-ray energies. For each SFS, $MTF_S(f)$ drops quickly in the range from 0 to 2 lp/mm due to the spread of x-ray energy deposition from the primary interaction site. Nevertheless, the $MTF_S(f)$ values of all SFSs remain high ($> 50\%$) beyond 25 lp/mm and are dominated by the 20 μm scintillating fiber diameter used. Table 1 summarizes the $MTF_S(f)$ values of all SFSs at 5, 10, 15 and 20 lp/mm spatial frequencies at 20 keV x-ray energy. However, at x-ray energies significantly higher than the K-or L-edges of the high Z elements, the $MTF_S(f)$ values were overestimated at high spatial frequency due to the increasing transverse range of the photoelectrons. This effect will be taken into account in the near future.

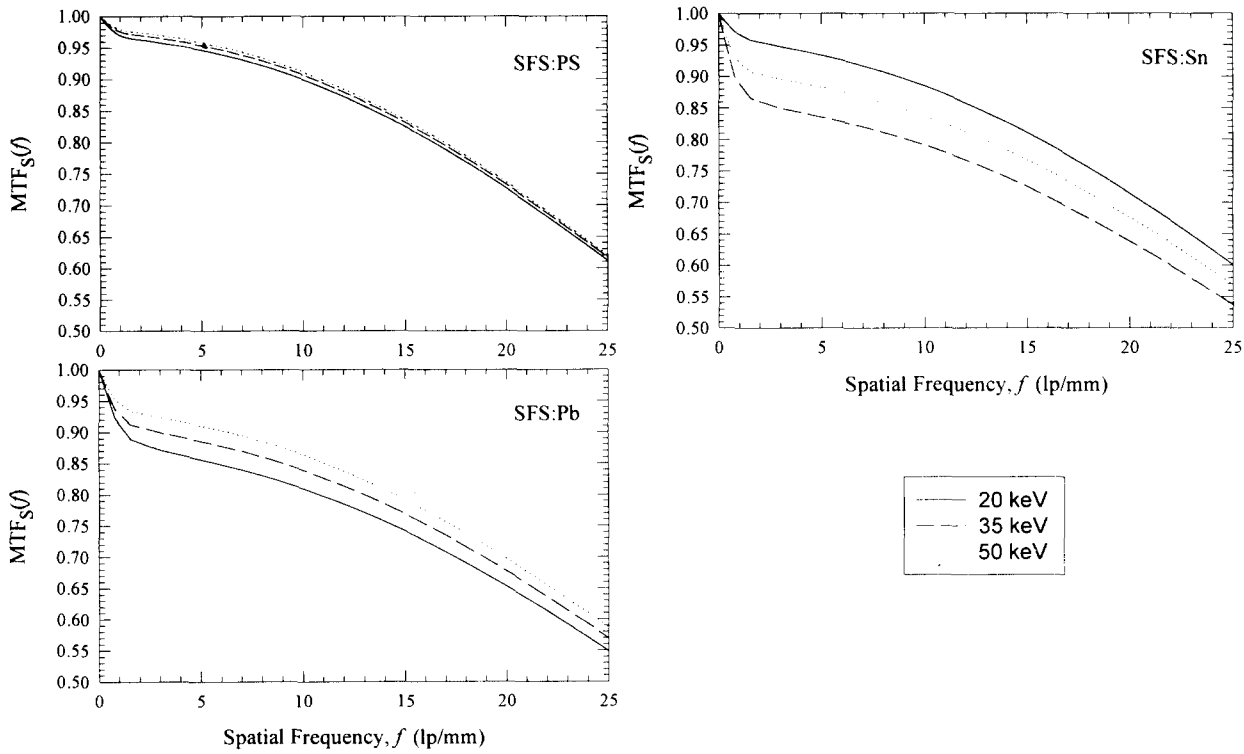

Fig. 8. MTF$_S$(f) curves of the three SFSs made of individual scintillating fibers of 20μm diameter at 20, 35, and 50 keV incident x-ray energies

Table 1. MTF$_S$(f) values at 20 keV incident x-ray energy

f (lp/mm)	MTF$_S$(f)		
	SFS : PS	SFS : Pb	SFS : Sn
5	0.94	0.85	0.93
10	0.90	0.81	0.89
15	0.82	0.74	0.81
20	0.73	0.65	0.72

CONCLUSION

We have investigated theoretically the effect of loading high Z element, lead and tin, on the zero spatial frequency detective quantum efficiency and modulation transfer function of a slot shaped plastic scintillating fiber screen in mammography. Loading high Z elements markedly improved the DQE(0) of the plastic SFS. DQE (0) of SFS : Pb is primarily determined by the SFS x-ray interaction efficiency, and is greater than 90% for a 2cm thick SFS at x-ray energies lower than 30 keV. For SFS : Sn, the DQE(0) is greater than 80% from 15 to 50 keV. The DQE(0) of a high Z element loaded SFS was found to be about a factor of three higher than the DQE(0) of an Min-R screen for mammography. At mammographic x-ray energies, MTF(f) values of all three SFSs are greater than 50% at 25 lp/mm spatial frequency, and dominated by the 20μm scintillating fiber diameter used in this analysis. The addition of high Z elements in the SFS showed little effect on the computed MTF(f) compared to the pure plastic SFS at x-ray energies used in mammography. The use of a high Z element loaded SFS in a scanning slot detector has the potential to provide a digital mammography system with both high detective quantum efficiency and excellent spatial resolution.

ACKNOWLEDGMENT

This work was supported by NASA and NIH under grants Nos. 1R01CA.65992-01, 1R41CA64988-01, and by the Department of The Army in the form of a predoctoral fellowship Grant (No. DAMD17-94-J-4058).

REFERENCES

1. A. D. A. Maidment, M. J. Yaffe, D. B. Plewes, G. M. Mawdsley, I. C. Soutar, B. G. Starkoski, "*Imaging performance of a prototype scanned-slot digital mammography system,*" Proc. SPIE 1896, pp. 93-103, 1993.
2. E. Toker and M. F. Piccaro, "*Design and development of a fiber optic TDI CCD-based slot-scan digital mammography system,*" Proc. SPIE 2009, July, 1993.
3. R. K. Swank, "*Absorption and noise in x-ray phosphors,*" J. Appl. Phys. 44, pp. 4199-4203, 1973.
4. R. K. Swank, "*Measurement of absorption and noise in an x-ray image intensifier,*" J. Appl. Phys. 45, pp. 3673-3678, 1974.
5. H. P. Chan and K. Doi, "*Studies of x-ray energy absorption and quantum noise properties of x-ray screens by use of Monte Carlo simulation,*" Med. Phys. 11(1), pp. 37-46, 1984.
6. C. E. Dick and J. W. Motz, "*Image information transfer properties of x-ray fluorescent screens,*" Med. Phys. 8, pp. 337-346, 1981.
7. Sandler and K. C. Tsou, "*Quenching of the Scintillation Process in Plastic by Organometallics,*" J. Phys. Chem. 68 (2), pp. 300-304, 1964.
8. W. Wunderly and J. M. Kauffman, "*New quench-resistant fluors for liquid scintillation counting,*" Appl. Radiat. Isot. Vol. 41, pp. 809-815, 1990.
9. J. F. Williamson, "*Monte Carlo Simulation of Photon Transport Phenomena : Sampling Techniques,*" Monte Carlo Simulation in the Radiological Sciences, R. L. Morin, pp. 53-101, CRC Press, Boca Raton, 1988
10. Technical Data TI0997 (2-89), Eastman Kodak Company, NY
11. D. P. Trauernicht and R. Van Metter, "*Conversion noise measurement for front and back x-ray intensifying screens,*" Proc. SPIE 1231, pp. 262-270, 1990.